metals

MDPI

Article

$Cu_{2-x}S$ and $Cu_{2-x}Se$ Alloys: Investigating the Influence of Ag, Zn, and Ni Doping on Structure and Transport Behavior

Andrzej Mikuła *, Tomasz Kurek, Miłosz Kożusznik and Paweł Nieroda

Faculty of Materials Science and Ceramics, AGH University of Krakow, al. Mickiewicza 30, 30-059 Krakow, Poland; qrek@agh.edu.pl (T.K.); mkozusznik@agh.edu.pl (M.K.); pnieroda@agh.edu.pl (P.N.)
* Correspondence: amikula@agh.edu.pl

Abstract: $Cu_{2-x}S$ and $Cu_{2-x}Se$ ($0 \leq x \leq 0.2$) alloys stand out as highly promising materials for thermoelectric applications, owing to the phonon–liquid electron–crystal (PLEC) convention. In this study, we undertake a comprehensive investigation to reassess the synthesis conditions, with a focus on achieving pure-phased systems through a direct reaction between elements at elevated temperatures. Simultaneously, we present experimental evidence showcasing the feasibility of doping these systems with Ag, Ni, and Zn. The study demonstrates that obtaining single-phased systems requires multi-step processes, and the dissolution of chosen impurities appears doubtful, as evidenced by numerous foreign phase segregations. Additionally, it is revealed that the partial dissolution of individual impurities deteriorates the operational parameters of these chalcogenides. For the optimal $Cu_{1.97}S$ composition, it reduces the thermoelectric figure-of-merit ZT from 1.5 to approximately 1.0, 0.65, and 0.85 for Ag-, Ni-, and Zn-doped systems, respectively, while marginally improving their stability. For metal-like $Cu_{1.8}Se$, the ZT parameter remains at a low level, ranging between 0.09 and 0.15, showing slight destabilization during subsequent operating cycles. The article concludes with an in-depth analysis of the basic thermoelectric performance exhibited by these doped systems, contributing valuable insights into the potential enhancements and applications of $Cu_{2-x}S$ and $Cu_{2-x}Se$ alloys in the field of thermoelectric materials.

Keywords: copper chalcogenides; transition-metal dopants; thermoelectric properties

Citation: Mikuła, A.; Kurek, T.; Kożusznik, M.; Nieroda, P. $Cu_{2-x}S$ and $Cu_{2-x}Se$ Alloys: Investigating the Influence of Ag, Zn, and Ni Doping on Structure and Transport Behavior. *Metals* **2024**, *14*, 360. https://doi.org/10.3390/met14030360

Academic Editor: Jan Vrestal

Received: 26 February 2024
Revised: 13 March 2024
Accepted: 18 March 2024
Published: 20 March 2024

1. Introduction

Copper(I) chalcogenides (Cu_2Ch) are among the promising mid- to high-temperature thermoelectric materials (TE) [1,2]. Phase diagrams of these compounds indicate a multitude of possible structures depending on the stoichiometry in individual sublattices and the available synthesis conditions [3–7]. According to the comprehensive study by Havlik [8], near the stoichiometry of Cu_2S, the most common room-temperature (RT) system is the so-called low-chalcocite characterized by a monoclinic structure. With slight deviations from stoichiometry, particularly in the Cu sublattice, an orthorhombic phase also occurs, exhibiting significantly better thermoelectric parameters [9], along with metastable tetrahedral and hexagonal phases. At higher temperatures, the low-symmetry variants of Cu_2S transition into the hexagonal and finally into the cubic phase. Similarly, in the case of copper(I) selenide, low-symmetry variations dominate at RT, transitioning into the β-phase—cubic form at higher temperatures [6,10–12]. Numerous documented examples also demonstrate the possibility of stabilizing this regular phase at RT [6,13–15]. The cubic forms of copper chalcogenides are particularly significant from the perspective of thermoelectric properties. In these structures, the large and relatively immobile chalcogen atoms create a crystalline pathway for charge carriers, simultaneously serving as scattering points for lattice phonons. On the other hand, the highly mobile copper ions exhibit liquid-like properties, facilitating rapid jumps between equivalent sites, providing an additional mechanism for phonon scattering, and ensuring a high ionic component of electrical conductivity [1,2,16–21]. In

the case of selenides, a high degree of structural disorder is also observed, contributing to a reduction in the lattice component of thermal conductivity [22]. In summary, the unique properties of these materials align with the concept of phonon–liquid electron–crystal (PLEC) conception, surpassing many other materials in terms of achieved thermoelectric figure-of-merit ZT parameter at the level of 1.9–2.1 at 1000 K [9,16]. Unfortunately, the temperature gradient, potential difference, and varying temperature conditions—natural working conditions for thermoelectric materials—result in the direct migration of copper ions. This leads to their accumulation on one side of the material, subsequently causing phase decomposition and deteriorating both mechanical and thermoelectric properties. This situation is exacerbated by the natural tendency to create vacancies in the Cu sublattice, which, in addition to the mentioned low stability, translates into the inherent affinity of these materials to function as p-type conductors. This poses difficulties in obtaining copper chalcogenides characterized by n-type conductivity [1,7,23–25]. Recently, various approaches have been suggested to improve the stability of Cu_2Ch-based compounds, encompassing the integration of nanoinclusions, doping procedures, the creation of multiphase systems, precise control of stoichiometry/crystal structure, and the application of temperature and vacuum treatment, either independently or in combination [26–35]. For instance, an exceptionally effective approach involved deliberately introducing foreign phases such as BiCuSeO, graphene, or carbon nanotubes into Cu_2Se, enabling the production of highly efficient materials with a ZT level of 2.0 [33–35]. All these methods aim to limit the formation of Cu vacancies and restrict the migration of Cu ions to local regions (e.g., within grains, but not across the entire material) by introducing suitable diffusion barriers in the form of foreign phases/inclusions. Especially relevant in this case appears to be the imposition of initial non-stoichiometry on the copper sublattice [9,36] or doping process [37,38], which may lead not only to better thermoelectric parameters but also to their increased durability.

This study focuses on the doping processes of $Cu_{2-x}Ch$ systems using Ag, Ni, and Zn. These elements are naturally occurring contaminants in copper ores exhibiting similar chemical properties. Consequently, they can be considered as both potential dopants and components of solid solution mixtures. The differences in size (especially in the case of silver) and the number of valence electrons can also lead to desired limitations of the excessive copper ion migration or result in electron-type conductivity, particularly in the case of Zn-doped systems. The available literature data for sulfides are severely limited in this regard, especially considering the approach of synthesizing such materials through classical reactions between elements under vacuum conditions. However, the literature does provide a few instances of Ag-doped $Cu_{2-x}S$ obtained through hydrothermal techniques [38]. In this scenario, even a relatively small addition of silver results in the formation of ternary compounds, such as CuAgS and copper(I) sulfide, with a deficiency in the Cu sublattice (e.g., $Cu_{1.96}S$) particularly noticeable after sintering. This implies the breakdown of the doped system or a reversible process of impurity dissolution at higher temperatures and resegregation at RT (similar to an Fe-doped system [39]). Examples of incorporating Ni or Zn as dopants into $Cu_{2-x}S$, with Ni/Zn substituting copper in a 1:1 ratio, are rarely documented in the literature. In cases where such examples exist, the procedures for obtaining them usually necessitate additional factors, such as pressure [40]. When Ni or Zn are mentioned as dopants, they usually exist in systems with a deficiency in the Cu sublattice, as seen in Ni-doped $Cu_{1.9}S$ [36]. Conversely, numerous instances showcase systems where Ni or Zn coexist with Cu in ternary and quaternary chalcogenides, which aligns with the inclination to form relatively stable multi-cationic phases with distinct structures rather than doped $Cu_{2-x}Ch$ [41,42]. Selenides appear to be much more susceptible to doping with these elements, especially in the case of Ag-doped systems. Similar to sulfides, even a doped system typically coexists with other phases, and literature reports on restricting copper ion migration through silver remain contradictory [1,25,31,43–48]. Ni and Zn also appear to be documented as dopants for Cu_2Se; however, the available literature base in this case is quite limited [13,14]. The paper provides a reassessment of the synthesis conditions'

impact on the feasibility of obtaining single-phased copper(I) sulfides and selenides. It also reevaluates the potential for doping these systems with Ag, Ni, and Zn. The analysis of structural parameters is consistently correlated with selected transport properties and stability issues, ensured through a series of cyclic measurements. The article concludes with an in-depth analysis of the basic thermoelectric performance exhibited by these doped systems, contributing a valuable insight into the potential enhancements and applications of $Cu_{2-x}S$ and $Cu_{2-x}Se$ alloys in the field of thermoelectric materials. Simultaneously, it provides a discussion in conjunction with the available literature on the subject.

2. Materials and Methods

The materials were obtained through high-temperature reaction between elements involving partial participation of the liquid phase, using 99.99% purity ingredients (Alfa Aesar) in the forms of powder (Cu, Ag, Ni, and Zn), shots (Se), and pieces (S). Appropriate amounts of each element were double-sealed in quartz tubes in vacuum conditions (10^2 Pa) and subjected to literature-based temperature treatment [9,13,49–53]. Initially, the materials were heated to 1273 K (selenides/sulfides) and 1073 K (sulfides) with a rate of 2 $Kmin^{-1}$ and subsequently annealed for 120 h, followed by quenching (immersion in tap water) or cooling to RT (5 $Kmin^{-1}$), maintaining relatively simple synthesis procedure. After a comprehensive structural analysis of the as-synthesized materials, selected compositions were ground in a mortar grinder (Retsch RM200) for 10 min and subjected to consolidation using Spark Plasma Sintering (SPS) technique, employing the following conditions: final temperature 773 K (100 $Kmin^{-1}$), pressure $50 \cdot 10^{-6}$ Pa, and Ar atmosphere.

The phase composition of the samples was examined via X-ray diffraction studies (XRD, PANanalytical Empyrean, Malvern Pananalytical Ltd., England, UK, CuKα radiation) and X'Pert HighScore (version 3.0d) software. Scanning electron microscopy (SEM) combined with energy-dispersive X-ray spectroscopy (EDX) was implemented to examine the microstructure and homogeneity of the samples (Thermo Scientific Fisher Phenom XL scanning electron microscope with EDX analyzer, ThermoFisher Scientific Inc., Carlsbad, CA, USA) in the forms of ingots/powders and sintered pellets. The thermal diffusivity (κ) of the materials was determined using the laser flash analysis method (LFA, NETZSCH LFA 427 analyzer, Netzsch, GER). By combining κ, specific heat C_p (determined from differential scanning calorimetry (DSC) measurements, NETZSCH STA 449 F3), and density ρ of the samples (determined based on hydrostatic Archimedes method, Table S1), the thermal conductivity (λ) of the materials was estimated (1). The thermal properties were assessed for sintered pellets with a thickness of 2–3 mm and a diameter of 10 mm.

$$\lambda = \kappa \cdot C_p \cdot \rho, \quad (1)$$

The total electrical conductivity (σ) and Seebeck coefficient (α) of the sintered materials were assessed using custom-made equipment employing the DC four-point method and Keysight electronic components. The samples for electrical measurements were examined in the form of cuboids with a square base (approximately 3 mm $\times$ 3 mm) and a length of about 6–8 mm. Such samples were cut from sintered pellets with a diameter of 15 mm and a density analogous to those used in thermal studies (Table S1). Resistance measurements were carried out with variable current polarization to eliminate the Seebeck voltage. Each measurement point represents the average of 3 separate measurements, with each individual measurement recording the resistance in both directions. The Seebeck coefficient was recorded with a temperature gradient of 3 K between the hot and cold sides of the sample. The measurements were conducted within a temperature range of 303–916 K, with a temperature increment of 10° and under an Ar atmosphere. Prior to each measurement, the temperature was stabilized for 35 min. Based on these measurements (α and σ) and incorporating the thermal conductivity, the thermoelectric figure of merit parameter, ZT,

was calculated—Equation (2). Additionally, the power factor (PF) was determined and presented in the Supplementary Materials Section (Figures S7 and S8).

$$ZT = \frac{\alpha^2 \cdot \sigma \cdot T}{\lambda}, \quad (2)$$

3. Results and Discussion

3.1. Structural Investigation—The Influence of Synthesis Conditions on Copper(I) Chalcogenide Phase Composition

Due to the reversible mechanism of the $Cu_{2-x}S$ phase transition that occurs during operating conditions, the synthesis procedure was limited to a single heating-cooling cycle. Both stoichiometric Cu_2S and copper sublattice non-stoichiometric $Cu_{1.97}S$ systems were considered, with $Cu_{1.97}S$ showing superior performance [9]. Based on the XRD measurements (Figure 1a), it is demonstrated that $Cu_{1.97}S$ predominantly consists of the desired djurleite phase characterized by orthorhombic structure, accompanied by a low content of low-chalcocite with a monoclinic structure, as evidenced by reflections at around 23.8, 28.2, and 37.5 as well as broadened reflections around 37.6 and 40.8 2θ. The coexistence of these two phases appears inevitable, particularly as their presence can be noticed after successive temperature cycles for all doped systems (see next sections) and the inability to distinguish them based on the microstructure observation (Figure S2). By decreasing the initial temperature synthesis to 1073 K, the main orthorhombic $Cu_{1.97}S$ phase is accompanied by a metastable, tetragonal phase (Figure 1a). Stoichiometric Cu_2S, in turn, indicates a pure-phased low-chalcocite structure regardless of the first step's annealing temperature (Figure 1b). Therefore, it seems that the current literature reports on the occurrence of low-temperature phases of $Cu_{2-x}S$ alloys after temperature treatment remain valid [5,9,53]. Due to the better TE properties of $Cu_{1.97}S$, this material was chosen for doping with selected metals.

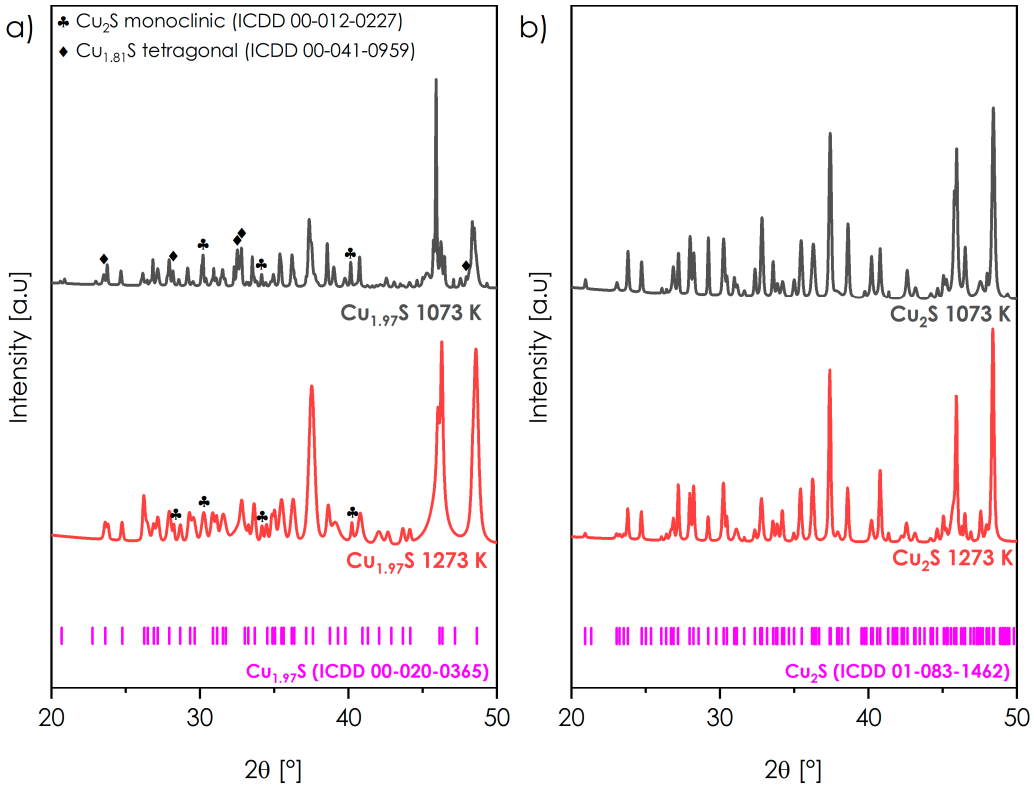

Figure 1. XRD diffraction patterns of copper(I) sulfides obtained by high-temperature reaction between elements and slow-cooled to RT from 1273 K or 1073 K: (**a**) $Cu_{1.97}S$, (**b**) Cu_2S.

The situation is different with $Cu_{2-x}Se$ (Figure 2). Literature suggests that it is possible to obtain a single-phased cubic structure and stabilize it at low temperatures by using hydrothermal techniques or through the quenching process [11,13]. However, in our work, the stoichiometric copper(I) selenide consistently appears as a mixture of two cubic phases (with nominal compositions of $Cu_{1.8}Se$ and Cu_2Se, respectively), regardless of whether the system underwent quenching or slow-cooling processes. For this reason, we investigated whether the deliberate induction of strong non-stoichiometry on the Cu sublattice, i.e., $Cu_{1.8}Se$, leads to achieving a pure-phased material. It has been found that by applying a slow-cooling approach, indeed, a single-phase material characterized by a cubic structure can be obtained, while the quenching process leads to achieving a mixture of cubic $Cu_{1.8}Se$ with precipitation of a metastable, tetragonal phase. Therefore, it can be concluded that employing the simplest synthesis routes leads to the most homogeneous systems, while rapid temperature change associated with quenching seems to disrupt the homogeneity of the selenide, only partially freezing the desired cubic $Cu_{2-x}Se$ phase. This is particularly important due to the cyclic nature of the operational conditions of TE materials (heating-cooling), which is often overlooked by many authors, neglecting to address the material's properties after subsequent cycles. Given the well-studied properties of doped Cu_2Se characterized by cubic structure [13,14,43,54], this study focuses on doping the single-phase $Cu_{1.8}Se$ system.

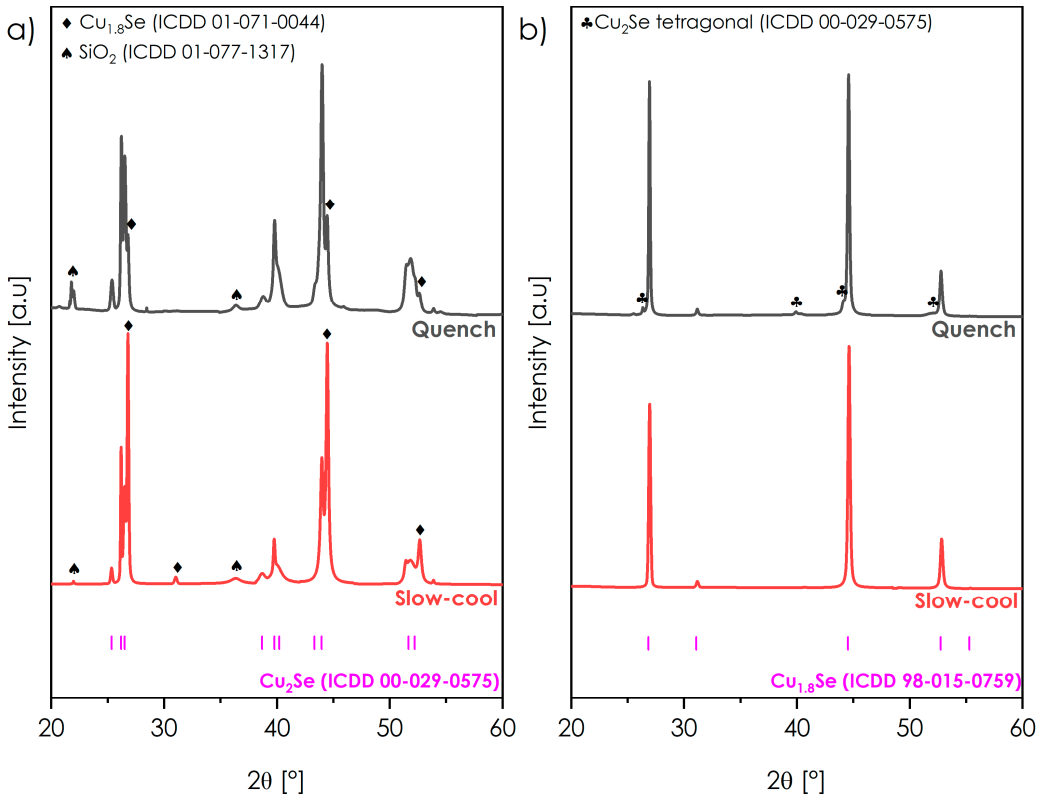

Figure 2. XRD diffraction patterns of copper(I) selenides obtained by high-temperature reaction between elements and slow-cooled or quenched to RT: (**a**) Cu_2Se, (**b**) $C_{1.8}Se$.

After sintering, the copper(I) sulfide, $Cu_{1.97}S$, completely transitioned into a monoclinic structure with significantly shifted respective reflections toward lower counts (Figure 3a), suggesting enlarged lattice parameters caused, most probably, by non-stoichiometry on the cationic sublattice (Table S2). It is also found that the (420) and (204) lattice facets are clearly dominant in this sample, as indicated by the enormous integral intensities of the reflections at about 32.5 and 35 2θ. It is difficult to interpret this result, as most available literature data do not present XRD patterns of materials before and after sintering. However, this

is doubly intriguing considering that the coexistence of two monoclinic phases differing by structure (chalcocite and djurleite) is present in both powders and sintered pellets of doped compounds (see next chapter). Sintering has no effect on the composition of non-stoichiometric $Cu_{1.8}Se$ (Figure 3b).

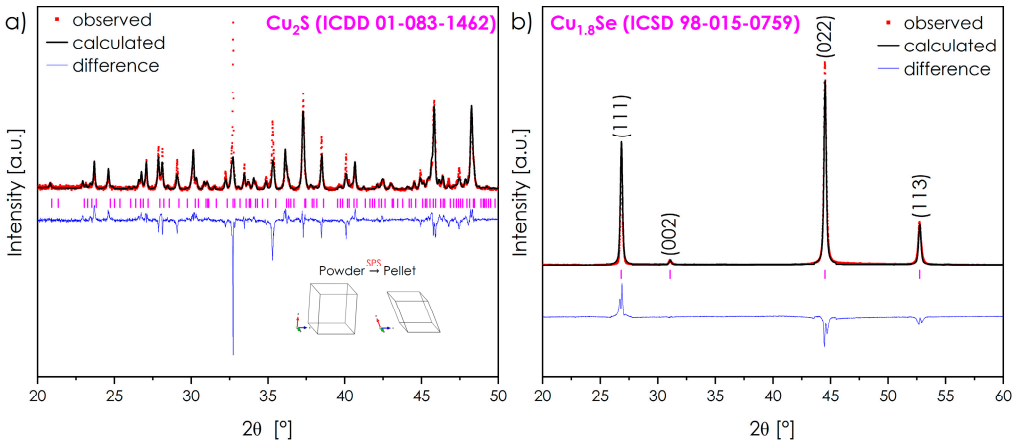

Figure 3. Rietveld analysis of sintered pellets: (**a**) $Cu_{1.97}S$; (**b**) $Cu_{1.8}Se$.

3.2. Structural Investigation—The Influence of Chosen Dopants on Phase Composition of $Cu_{2-x}Ch$

The effect of dopants on phase composition and chemical homogeneity of $Cu_{1.97-x}M_xS$ and $Cu_{1.8-x}M_xSe$ were assessed again by XRD studies coupled with microstructure observations (Figures S1–S4). The diffractograms of the sulfides after SPS sintering differed markedly from those obtained before the condensation process (Figure 4). For $Cu_{1.96}Ag_{0.01}S$ and $Cu_{1.96}Ni_{0.01}S$, the dominant phase is chalcocite characterized by a monoclinic structure, with the addition of a second, monoclinic $Cu_{31}S_{16}$ (djurleite). The presence of these two phases, once again, suggests the formation of a solid solution with similar symmetry but differing in lattice parameters. However, it remains an open question whether one of these phases is rich in dopants affecting the lattice size or the effect of a non-uniform temperature gradient during annealing. As-synthesized materials do not exhibit inclusions of other phases, indicating that the dopants may undergo partial dissolution during the synthesis procedure. However, the SPS consolidation leads to the disappearance of some reflections and changes in the integral intensities of other ones, suggesting an increased contribution of the chalcocite phase, accompanied by the disappearance of the djurleite phase. At the same time, precipitations of foreign phases rich in Ag and Ni appear, whose presence is further confirmed by SEM+EDX analysis (Figures S1 and S2). Only $Cu_{1.96}Zn_{0.01}S$ shows the characteristics of a single-phase material (with a preserved tendency toward an increased contribution of the orthorhombic phase after SPS), suggesting that Zn doping is the only one that at least partially incorporates into the copper(I) sulfide structure during the preparation process. Notably, a single reflection that should be attributed to the residual presence of metastable tetragonal $Cu_{1.96}S$ is also observed in the Zn-doped sulfide diffractogram.

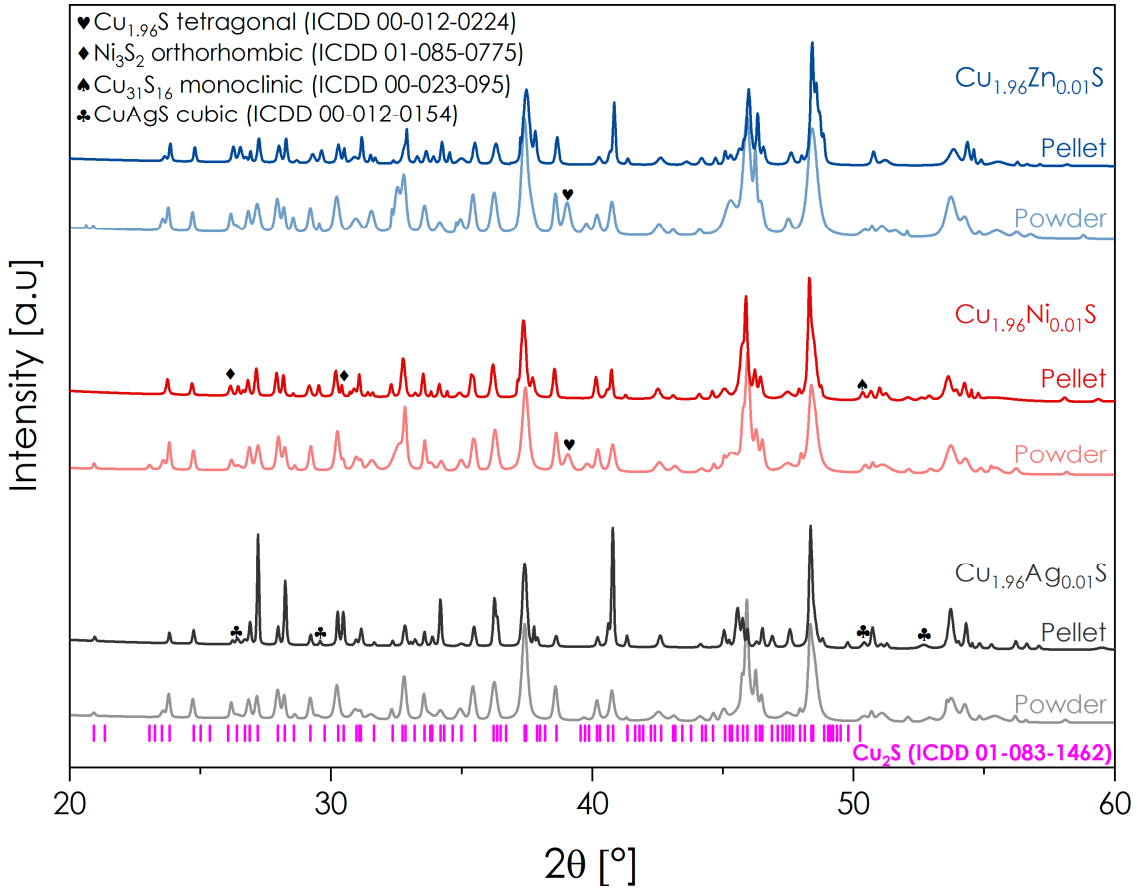

Figure 4. The comparison of powder and sintered pellet XRD diffraction patterns of $Cu_{1.96}M_{0.01}S$ (M = Ag, Ni, Zn).

Surprisingly, in the case of selenides, doped materials after synthesis indicate the presence of a cubic $Cu_{1.8}Se$ phase with the additional presence of a residual tetragonal phase with a nominal formula Cu_3Se_2 (Figure 5). Taking into account the positions of the main reflections from this residual phase, which follow the sizes of individual ions (Ag > Zn > Ni), it can be presumed that this phase is rich in impurities. At the same time, the absence of foreign phases associated with dopant metals can be observed, indicating at least partial dissolution of these dopants in the selenide structure. The same observation can be made on the basis of microstructure observations, where only rare Ag-rich areas can be noticed (Figure S3). The presence of the tetragonal phase diminishes during consolidation processes, confirming phase homogenization during sintering, simultaneously shifting the reflections related to cubic $Cu_{1.8}Se$ noticeably toward lower angles. These shifts can be attributed to several phenomena, starting from the relaxation of the materials during sintering processes to successful doping processes resulting in increased unit cell parameters. Since the potential incorporation of Ni and Zn into β-Cu_2Se does not indicate such strong shifts in reflections, especially for Ni doping, which should affect the shifting of analogous reflections toward higher angles [13], another explanation suggests itself. The dopants dissolve in the tetragonal phase, and during the sintering process, they undergo segregation, leading to the homogenization of the main phase into pure-phase $Cu_{1.8}Se$. Despite the apparent phase homogeneity, processes of segregation of dopant-rich phases can be seen on SEM images. This is particularly evident for the $Cu_{1.79}Ag_{0.01}Se$ pellet, where the diffraction pattern indicates the presence of Ag_2Se, also visible in the SEM images (Figure S4). Once again, the only admixture that probably successfully incorporates into the $Cu_{1.8}Se$ structure is Zn.

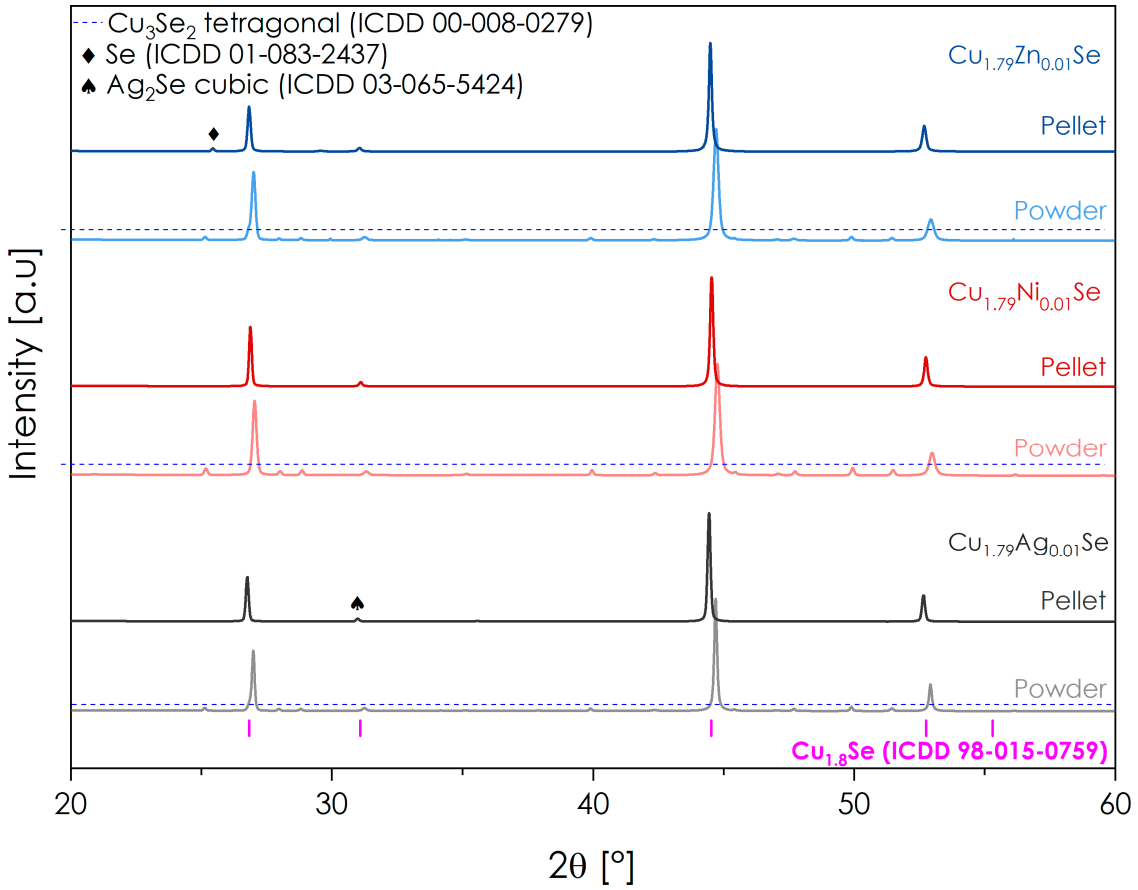

Figure 5. The comparison of powder and sintered pellet XRD diffraction patterns of $Cu_{1.79}M_{0.01}Se$ (M = Ag, Ni, Zn).

3.3. Transport Properties of Undoped and Doped $Cu_{2-x}Ch$ Systems

The selected materials for further investigation, both undoped ($Cu_{1.97}S$ and $Cu_{1.8}Se$) and doped, were subjected to transport studies. The thermal conductivity λ of the non-stoichiometric sulfide (Figure 6a) oscillates around 0.45 $Wm^{-1}K^{-1}$ at RT and remains relatively constant at approximately 0.4–0.5 $Wm^{-1}K^{-1}$ across the entire range of analyzed temperatures. Two distinct peaks at temperatures around 350 and 530 K correspond to phase transitions occurring in this system. Both the total thermal conductivity value and the significant contribution of the lattice component (Figure S5) are comparable to the lowest values found in the literature for $Cu_{1.97}S$ or Cu_2S [9,53]. The presence of dopants, whether partially dissolved or as copper sulfide with metallic precipitation or the presence of foreign phases rather unfavorably affects the thermal properties of this material. The addition of silver as a dopant, as long as it occurs without the presence of foreign phases, increases the electronic component of conductivity but slightly reduces thermal conductivity due to the additional phonon scattering centers. The coexistence of the doped system with a ternary chalcogenide further enhances the electronic component and increases the total thermal conductivity [38]. We obtained a similar effect, recording the total thermal conductivity in the range of 0.6–0.7 $Wm^{-1}K^{-1}$, which, however, remains a better result than the Ag-doped one presented by Yue et al. [38]. The addition of Ni dopant almost doubles the total thermal conductivity value compared to the undoped material, primarily due to a significantly increased contribution of the lattice component. This result contradicts the findings of Shen et al. [36], who observed a decrease in both the lattice component and the total thermal conductivity for Ni-doped $Cu_{1.9}S$. However, in the cited study, this effect was associated with the presence of nanopores that appeared in the system upon the addition of nickel, which is not observed in our work. Therefore, the presence of inclusions seems to be crucial

here. Additionally, an intriguingly strong thermal effect was observed at around 470 K. This behavior is highly unusual, as a significant decrease in both thermal diffusivity and specific heat were recorded, which were measured independently. While the potential oxidation of Ni-rich precipitations into nickel oxides, as observed in SEM images (Figure S4), is a consideration, it fails to account for the observed rise in thermal conductivity at elevated temperatures. This phenomenon demands further comprehensive exploration and remains largely unresolved within the scope of this study. For the Zn dopant, an almost threefold increase in thermal conductivity is observed, which is associated with both an increase in the electronic and lattice components and should be attributed to at least partial dissolution of this dopant in the structure. Thus, the formation of doped sulfide or heterostructures in this system significantly unfavorably affects the thermal properties of copper sulfide.

The thermal conductivity of copper(I) selenide characterized by the $Cu_{1.8}Se$ formula recorded in this study exhibits very high values at around 8 $Wm^{-1}K^{-1}$ at RT and decreases with temperature to approximately 4.5 $Wm^{-1}K^{-1}$ at 450 K (Figure 6b). This result indicates the material's highly metallic properties with a very high electronic component, reaching a value around 4–5 $Wm^{-1}K^{-1}$ across the entire temperature range (Figure S6). This result is significantly higher than those recorded for stoichiometric Cu_2Se at around 2 $Wm^{-1}K^{-1}$ [22] or even $Cu_{1.8}Se$ obtained via mechanical alloying, where conductivity around 5 $Wm^{-1}K^{-1}$ was reported [55]. This finding is remarkable, considering the relatively low density of the obtained materials (Table S1). The higher thermal conductivity, in this case, is due to the relatively low degree of disorder resulting from copper sublattice deficiency, which leads to reduced lattice components in stoichiometric material [12], relatively large grains compared to those obtained by Ji et al. via mechanical alloying [55], and the aforementioned highly metallic character of the sample. Also, in this case, the presence of dopants does not positively affect the thermal parameters of the material (Figure 6b), which is especially surprising for silver dopants, as according to the literature, both Ag doping and the presence of foreign Ag-rich phases should significantly reduce the lattice component of λ [37]. Meanwhile, the only dopant that significantly affects the reduction of the lattice component and total λ (particularly in high-temperature regions) is zinc, confirming our earlier statements that it is probably the only dopant that incorporates into the structure of this material providing additional centers for lattice phonons scattering. Furthermore, this material also exhibits a reduction in the λ_e, which is confirmed by studies on zinc doping of the stoichiometric system [13,14,54]. Slightly reduced λ_e and total λ were also expected for nickel doping [13]. However, we obtained opposite results, probably due to the presence of metallic precipitations. Thus, similar to the case of copper(I) sulfide, the systems containing segregation of foreign phases unfavorably affect the thermal parameters of copper selenide.

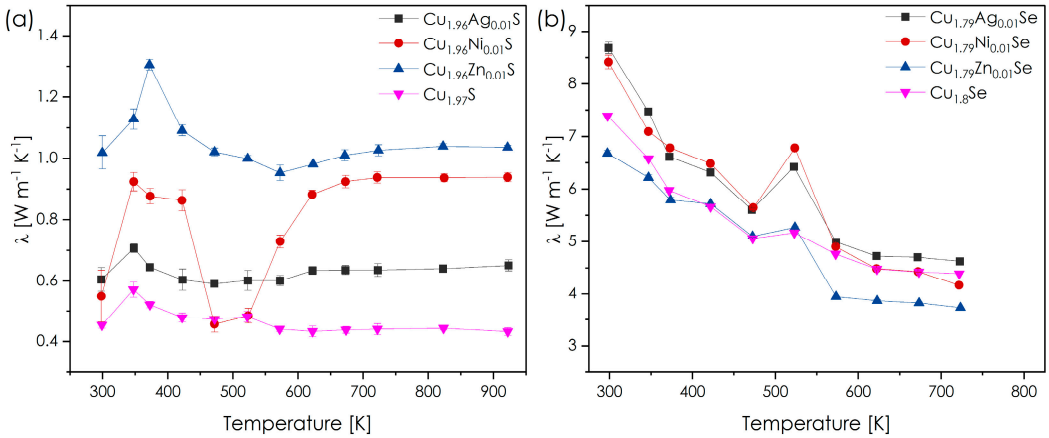

Figure 6. Thermal conductivity of undoped and doped copper chalcogenides as a function of temperature: $Cu_{1.97}S$ (**a**); $Cu_{1.8}Se$ (**b**).

Electrical measurements, including electrical conductivity σ and Seebeck coefficient α, were conducted in a cyclic mode to demonstrate the stability or potential relaxation processes of these materials under operating conditions (Figures 7–10). The Seebeck coefficient of undoped $Cu_{1.97}S$ is around 100 μVK^{-1} at RT and increases to approximately 300 μVK^{-1} at 900 K, exhibiting two anomalies consistent with phase transitions and characteristic behavior for degenerate p-type semiconductors (Figure 7). These values are slightly lower than those of stoichiometric Cu_2S and similar to those obtained in other studies on this material [9,53]. The stability of this material in successive measurement cycles also appears to be good, as indicated by minor deviations in individual measurements as a function of temperature and cycles. The introduction of Ag, Ni, and Zn induces marginal changes in this parameter, both in terms of achieved values and repeatability (Figure 7). The addition of silver slightly increases α, presumably due to a decrease in charge carrier mobility (affected by Ag dopant/Ag-rich phases and increased structure disordering), which, however, was not observed in the work of Yue et al. [38]. An even smaller increase in achieved Seebeck coefficient values is observed for nickel doping. Both of these effects are difficult to classify due to the presence of foreign phases but suggestively are related to a decrease in charge carrier concentration. On the other hand, the presence of metallic segregation or partial dissolution of zinc in copper sulfide leads to a decrease in the observed values of α, presumably due to the opposite effect, namely an increase in charge carrier concentration. A strong effect associated with a phase transition in the temperature range of 400–550 K is not observed in the Seebeck coefficient curves.

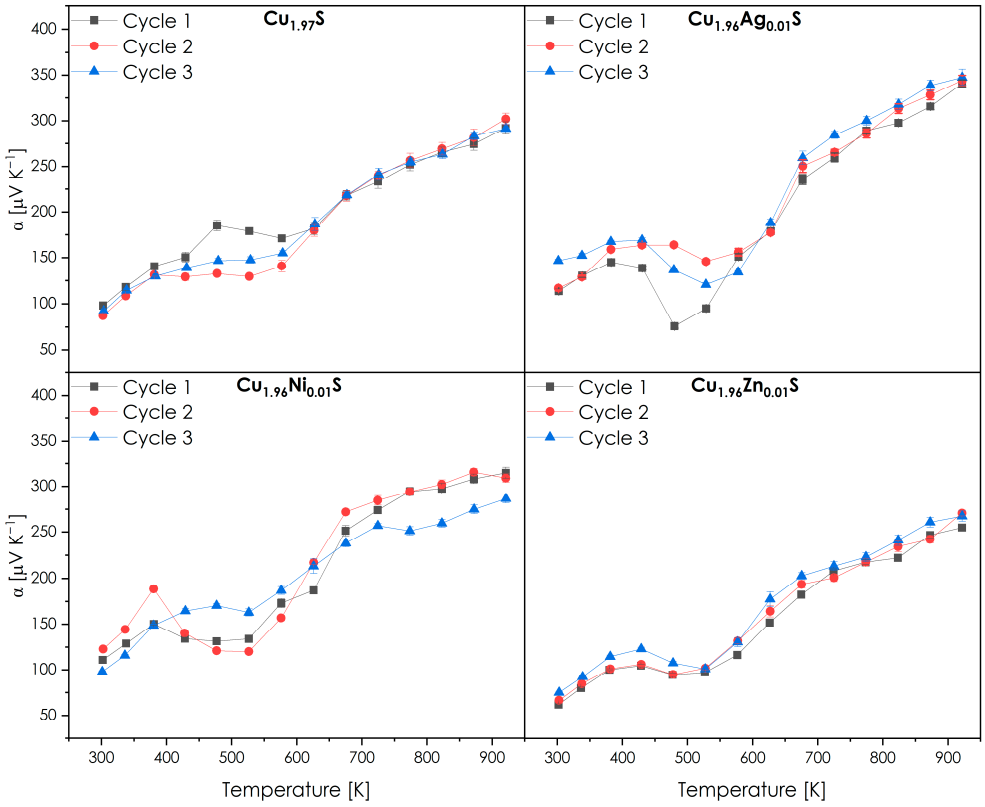

Figure 7. Seebeck coefficient as a function of temperature for copper(I) sulfide systems.

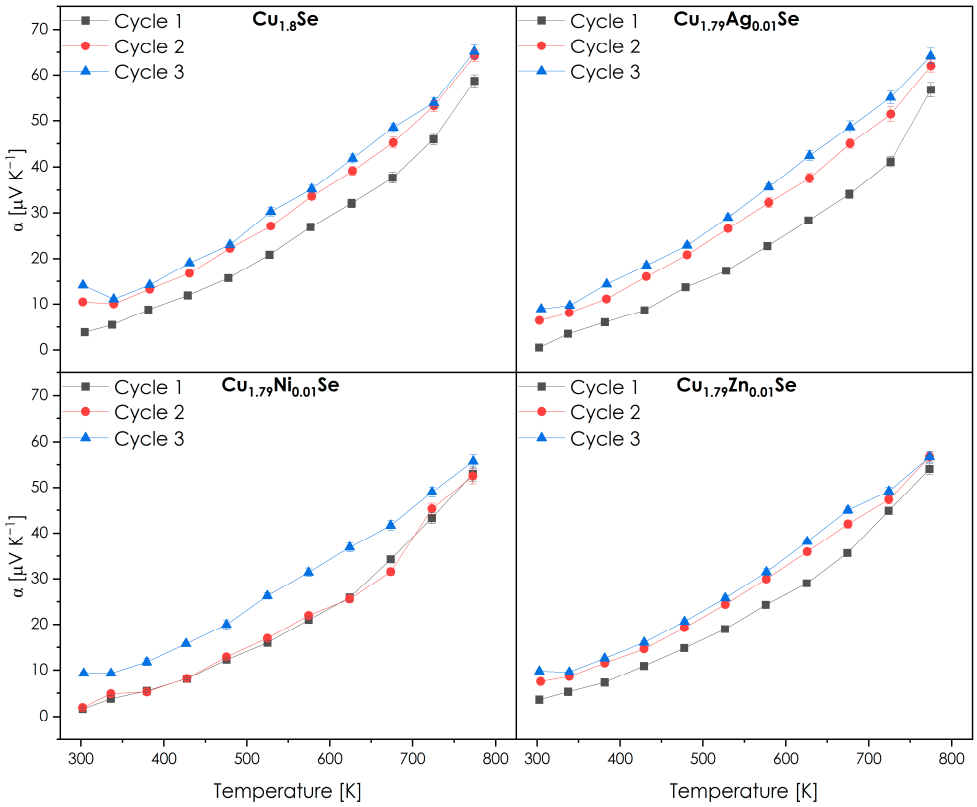

Figure 8. Seebeck coefficient as a function of temperature for copper(I) selenide systems.

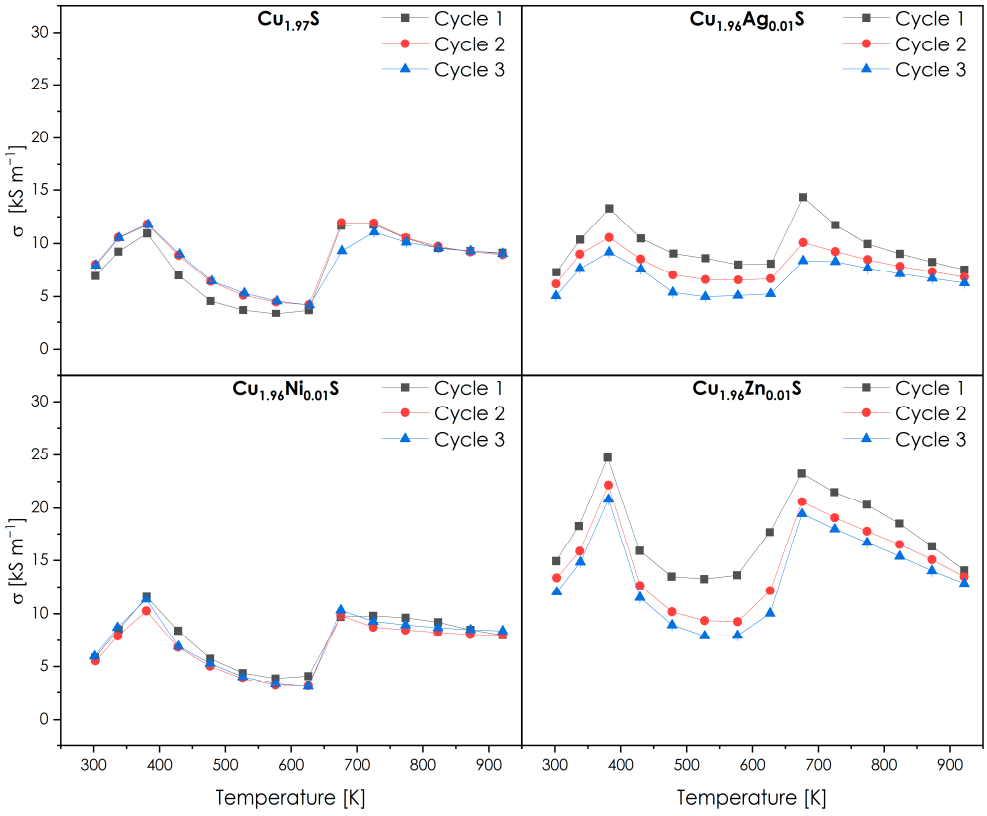

Figure 9. Electrical conductivity as a function of temperature for copper(I) sulfide systems.

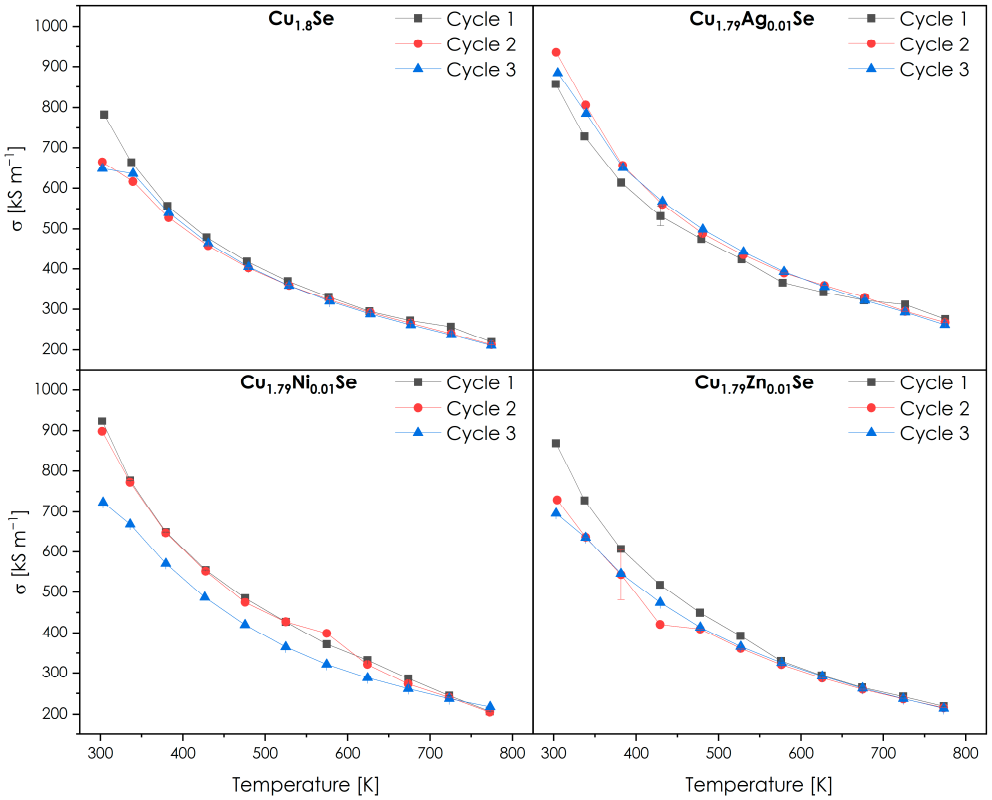

Figure 10. Electrical conductivity as a function of temperature for copper(I) selenide systems.

Similar to thermal conductivity, the strongly metallic character of copper selenide is also observed in the values of the Seebeck coefficient (Figure 8). This parameter takes values around 10 μVK^{-1} at RT and increases practically linearly to around 60–70 μVK^{-1} at 750 K. The presence of dopants and/or additional phases has a similarly marginal effect here, with a tendency for lower α values for doped systems (Figure 8). This may be associated with both an increase in charge carrier concentration and further defect formation in the cationic sublattice with successive measurement cycles, suggesting significantly lower stability of $Cu_{1.8}Se$ than $Cu_{1.97}S$. Once again, this result contradicts literature reports, where zinc or nickel dopants result in an increase in recorded Seebeck coefficient values [13,54]. However, there is a possibility that this slight decrease should be correlated with an increasing contribution of minority charge carriers. Nickel and zinc can act as electron donors here, masking the effects related to total Seebeck coefficient values.

The electrical conductivity σ of $Cu_{1.97}S$ systems (Figure 9) reaches values around 10^4 Sm^{-1} with a clear tendency to decrease in the temperature range of 400–600 K, corresponding to the presence of the $Cu_{1.96}S$ phase with a tetragonal structure [9]. In the case of undoped material, the electrical conductivity is a repeatable value in successive measurement cycles, with a slight tendency to improve this parameter. The electrical conductivity curve of Ni-doped material exhibits a similar trend. However, the addition of silver and zinc significantly deteriorates the σ of these materials with successive measurement cycles (Figure 9). This is interesting because there is no simultaneous increase in the Seebeck coefficient, which may have several reasons. The first is the dissolution of the dopants during measurements, leading to a decrease in charge carrier mobility. However, a more probable explanation is the further segregation of foreign phases, which does not affect the recorded values of α but affects the conductivity abilities, for example, through precipitation and partial oxidation of metal-rich phases at grain boundaries. The possibility of decreased electrical conductivity in subsequent cycles could also be attributed to charge accumulation at the grain boundaries, which is caused by the significant ionic contribution to electrical conductivity. Still, the electrical conductivity recorded in the presented study is one order

of magnitude higher than those shown by Yue et al. [38]. We do not observe such effects in the case of $Cu_{1.8}Se$ selenide (Figure 10). The strongly metallic character of these materials (doped and undoped) is evident here, with achieved values on the order of 10^5 or even 10^6 Sm^{-1} at RT and a typical decrease in conductivity with increasing temperature, which is a characteristic of metals. These results are significantly higher than those presented by various dopants (including Ni and Zn) in β-Cu_2Se [13] and nearly twice the values of those presented by Nieroda for the stoichiometric Cu_2Se obtained via the hydrothermal method [11]. It is worth noting the slightly higher conductivity values for Ni-doped $Cu_{1.8}Se$ compared to the undoped system, which is unusual considering that nickel should be a donor dopant. This situation is most likely associated with the increased charge carrier concentration provided by the dopant as well as the presence of metallic precipitates at grain boundaries. The differences in recorded values between individual measurement cycles are negligible for all considered compositions.

It should be underlined here that all considered samples (both doped $Cu_{1.97}S$ and $Cu_{1.8}Se$), despite preserved chemical (with an absence of free Cu precipitations) and phase compositions, exhibit a minor macroscopic deformation during TE operating (Figure S9). This implies real limitations in the application of $Cu_{2-x}Ch$ systems and raises questions regarding the available literature data.

After combining the above-described transport properties, the ZT parameter was determined as a function of temperature and individual measurement cycles (Figures 11 and 12). For sulfides, the highest recorded value of about 1.5 is achieved by undoped $Cu_{1.97}S$ at 923 K, which stays in line with available literature data [9,56] (Figure 11). All introduced dopants lead to a significant deterioration of this parameter, with minor changes in the profiles over individual cycles. An exception is the Ni dopant, for which a nearly half reduction in ZT is noticed in the third cycle compared to the first one, primarily due to the recorded Seebeck coefficient values, particularly in the high-temperature ranges. This result also contradicts similar systems, where the addition of Ni, whether incorporated or precipitated as a foreign phase, consistently leads to an increase in the final ZT values [36].

ZT parameter for metal-like $Cu_{1.8}Se$ exhibits very low values at around 0.09 for the first cycle and approximately 0.115 for the third cycle at temperature 723 K, which remains nearly fifteenfold lower than that for Cu_2Se reported in the literature [11–13] (Figure 12). In this case, the presence of dopants does not result in a deterioration of the ZT parameter; on the contrary, it rather improves ZT, showing increasingly better properties with each subsequent cycle, suggesting material relaxation during operating conditions. However, these materials still remain a relatively poor group of candidates for thermoelectric applications, unlike the indications from the literature for doped Cu_2Se [13,43,54].

Generally, it appears that precise control of stoichiometry is a much more effective approach for obtaining stable TE materials for these systems than introducing dopants or small amounts of foreign phases. The mentioned approach begins to yield satisfactory results only with the intentional and deliberate presence of other phases or chalcogenide-based composites [29,57].

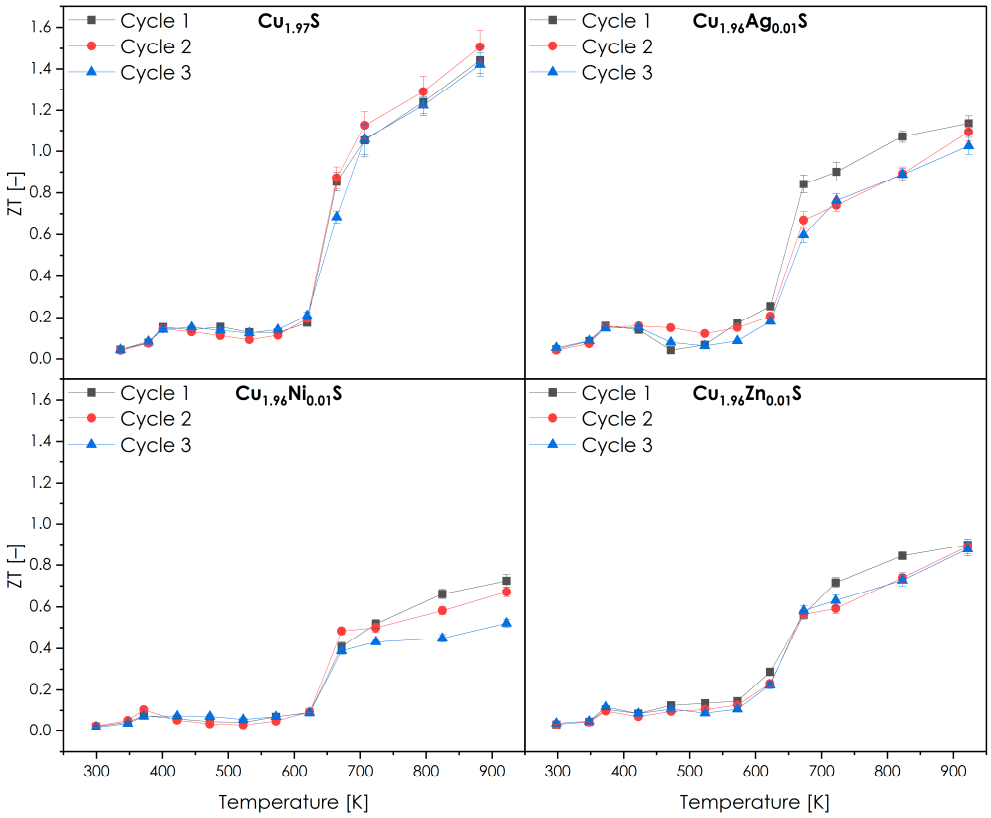

Figure 11. Thermoelectric figure of merit parameter ZT as a function of temperature for copper(I) sulfide systems.

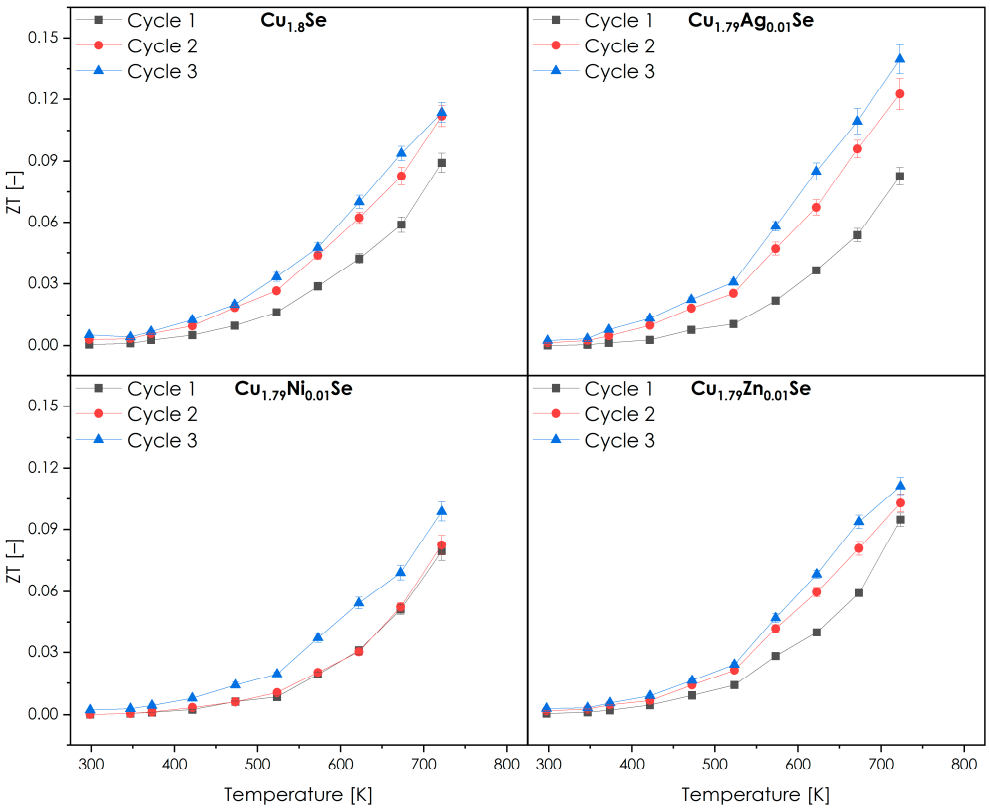

Figure 12. Thermoelectric figure of merit parameter ZT as a function of temperature for copper(I) selenide systems.

4. Conclusions

The presented study aimed to reassess the potential for synthesizing materials based on copper(I) chalcogenides, using a direct reaction between elements. It was demonstrated that employing a relatively simple annealing–cooling scheme can yield materials with the desired phase compositions. However, the most promising material characterized by the nominal composition of $Cu_{1.97}S$ remains a mixture of phases, while copper selenide exhibits single-phase behavior only in strongly non-stoichiometric systems such as $Cu_{1.8}Se$. In the subsequent sections of the paper, the focus was on attempts to dope these two non-stoichiometric chalcogenides. It was also shown that Ag, Ni, and Zn dopants indicate very limited solubility in these structures, which leads to obtaining multiphase systems, except for zinc. However, incorporating zinc into these chalcogenides has adverse effects on the thermoelectric performance due to its increasingly metallic character. Other dopants also worsen operational properties, marginally improving the repeatability of individual measurements. Moreover, all doped systems undergo macroscopic deformation, which, combined with poorer performance, disqualifies them as an effective means of modifying the thermoelectric properties of copper(I) chalcogenides. Thus, we demonstrated that controlling stoichiometry is a better approach, in the case of copper chalcogenides, for achieving a good thermoelectric material than doping or introducing small amounts of foreign phases. Therefore, non-stoichiometric $Cu_{1.97}S$, characterized by the highest ZT value of 1.5 and relatively good stability, remains one of the best materials for potential thermoelectric applications.

Supplementary Materials: The following supporting information can be downloaded at https://www.mdpi.com/article/10.3390/met14030360/s1, Figure S1: SEM micrographs together with EDX map analysis of $Cu_{1.97-x}M_xS$ (M = Ag, Ni, Zn; x = 0, 0.01) ingots; Figure S2: SEM micrographs together with EDX map analysis of $Cu_{1.97-x}M_xS$ (M = Ag, Ni, Zn; x = 0, 0.01) pellets; Figure S3: SEM micrographs together with EDX map analysis of $Cu_{1.8-x}M_xSe$ (M = Ag, Ni, Zn; x = 0, 0.01) ingots; Figure S4: SEM micrographs together with EDX map analysis of $Cu_{1.8-x}M_xSe$ (M = Ag, Ni, Zn; x = 0, 0.01) pellets; Figure S5: Lattice and electronic components of thermal conductivity as a function of temperature for copper(I) sulfides; Figure S6: Lattice and electronic components of thermal conductivity as a function of temperature for copper (I) selenides; Figure S7: Power factor as a function of temperature for copper(I) sulfides; Figure S8: Power factor as a function of temperature for copper(I) selenides; Figure S9: Optical microscope images of $Cu_{1.97}S$ and $Cu_{1.8}Se$ after TE measurements; Table S1: Density of undoped and doped copper(I) chalcogenide sinters; Table S2: Lattice constants and goodness of fit parameters for $Cu_{1.97}S$ and $Cu_{1.8}Se$ materials.

Author Contributions: Conceptualization, A.M.; methodology, A.M. and P.N.; validation, A.M.; formal analysis, A.M.; investigation, A.M., T.K., M.K. and P.N.; resources, A.M.; data curation, T.K., M.K., and P.N.; writing—original draft preparation, A.M., T.K. and M.K.; writing—review and editing, A.M.; visualization, T.K. and M.K.; supervision, A.M.; project administration, A.M.; funding acquisition, A.M. All authors have read and agreed to the published version of the manuscript.

Funding: This research was partially supported by the program "Excellence Initiative—Research University" for the AGH University of Krakow, grant ID 4752. T.K., M.K. and P.N. acknowledges the financial support of the Polish Ministry of Education and Science within the framework of Subvention for Science 2023.

Data Availability Statement: The data presented in this study are available on request from the corresponding author. The data are not publicly available due to privacy restrictions.

Conflicts of Interest: The authors declare no conflicts of interest.

References

1. Qiu, P.; Shi, X.; Chen, L. Cu-Based Thermoelectric Materials. *Energy Storage Mater.* **2016**, *3*, 85–97. [CrossRef]
2. Liu, H.; Shi, X.; Xu, F.; Zhang, L.; Zhang, W.; Chen, L.; Li, Q.; Uher, C.; Day, T.; Snyder, G.J. Copper Ion Liquid-like Thermoelectrics. *Nat. Mater.* **2012**, *11*, 422–425. [CrossRef] [PubMed]
3. Yu, X.; An, X. Controllable Hydrothermal Synthesis of Cu_2S Nanowires on the Copper Substrate. *Mater. Lett.* **2010**, *64*, 252–254. [CrossRef]

4. Blachnik, R.; Müller, A. The Formation of Cu_2S from the Elements II. Copper Used in Form of Foils. *Thermochim. Acta* **2001**, *366*, 47–59. [CrossRef]
5. Grønvold, F.; Westrum, E.F. Thermodynamics of Copper Sulfides I. Heat Capacity and Thermodynamic Properties of Copper(I) Sulfide, Cu_2S, from 5 to 950 K. *J. Chem. Thermodyn.* **1987**, *19*, 1183–1198. [CrossRef]
6. Tyagi, K.; Gahtori, B.; Bathula, S.; Jayasimhadri, M.; Sharma, S.; Singh, N.K.; Haranath, D.; Srivastava, A.K.; Dhar, A. Crystal Structure and Mechanical Properties of Spark Plasma Sintered Cu_2Se: An Efficient Photovoltaic and Thermoelectric Material. *Solid. State Commun.* **2015**, *207*, 21–25. [CrossRef]
7. Brown, D.R.; Day, T.; Borup, K.A.; Christensen, S.; Iversen, B.B.; Snyder, G.J. Phase Transition Enhanced Thermoelectric Figure-of-Merit in Copper Chalcogenides. *APL Mater.* **2013**, *1*, 052107. [CrossRef]
8. Havlík, T. Phase Equilibrium of Copper Iron Sulphides. In *Hydrometallurgy*; Elsevier: Amsterdam, The Netherlands, 2008; pp. 29–59.
9. Zhao, L.; Wang, X.; Fei, F.Y.; Wang, J.; Cheng, Z.; Dou, S.; Wang, J.; Snyder, G.J. High Thermoelectric and Mechanical Performance in Highly Dense $Cu_{2-x}S$ Bulks Prepared by a Melt-Solidification Technique. *J. Mater. Chem. A* **2015**, *3*, 9432–9437. [CrossRef]
10. Lu, P.; Liu, H.L.; Yuan, X.; Xu, F.F.; Shi, X.; ZHao, K.P.; Qiu, W.J.; Zhang, W.Q.; Chen, L.D. Multiformity and Fluctuation of Cu Ordering in Cu_2Se Thermoelectric Materials. *J. Mater. Chem. A Mater. Energy Sustain.* **2015**, *3*, 6901–6908. [CrossRef]
11. Nieroda, P.; Kusior, A.; Leszczyński, J.; Rutkowski, P.; Koleżyński, A. Thermoelectric Properties of Cu_2Se Synthesized by Hydrothermal Method and Densified by SPS Technique. *Materials* **2021**, *14*, 3650. [CrossRef] [PubMed]
12. Kim, H.; Ballikaya, S.; Chi, H.; Ahn, J.-P.; Ahn, K.; Uher, C.; Kaviany, M. Ultralow Thermal Conductivity of β-Cu_2Se by Atomic Fluidity and Structure Distortion. *Acta Mater.* **2015**, *86*, 247–253. [CrossRef]
13. Peng, P.; Gong, Z.N.; Liu, F.S.; Huang, M.J.; Ao, W.Q.; Li, Y.; Li, J.Q. Structure and Thermoelectric Performance of β-Cu_2Se Doped with Fe, Ni, Mn, In, Zn or Sm. *Intermetallics* **2016**, *75*, 72–78. [CrossRef]
14. Qin, Y.; Yang, L.; Wei, J.; Yang, S.; Zhang, M.; Wang, X.; Yang, F. Doping Effect on Cu_2Se Thermoelectric Performance: A Review. *Materials* **2020**, *13*, 5704. [CrossRef]
15. Li, L.; Zhao, Y.; Shi, C.; Zeng, W.; Liao, B.; Zhang, M.; Tao, X. Facile Synthesis of Copper Selenides with Different Stoichiometric Compositions and Their Thermoelectric Performance at a Low Temperature Range. *RSC Adv.* **2021**, *11*, 25955–25960. [CrossRef]
16. Zhao, K.; Qiu, P.; Shi, X.; Chen, L. Recent Advances in Liquid-Like Thermoelectric Materials. *Adv. Funct. Mater.* **2020**, *30*, 1903867. [CrossRef]
17. Mao, T.; Qiu, P.; Hu, P.; Du, X.; Zhao, K.; Wei, T.; Xiao, J.; Shi, X.; Chen, L. Decoupling Thermoelectric Performance and Stability in Liquid-Like Thermoelectric Materials. *Adv. Sci.* **2019**, *7*, 1901598. [CrossRef] [PubMed]
18. Wang, L. High Chalcocite Cu_2S: A Solid-Liquid Hybrid Phase. *Phys. Rev. Lett.* **2012**, *108*, 085703. [CrossRef] [PubMed]
19. Danilkin, S.A.; Avdeev, M.; Sale, M.; Sakuma, T. Neutron Scattering Study of Ionic Diffusion in Cu–Se Superionic Compounds. *Solid State Ion.* **2012**, *225*, 190–193. [CrossRef]
20. Liu, H.; Yuan, X.; Lu, P.; Shi, X.; Xu, F.; He, Y.; Tang, Y.; Bai, S.; Zhang, W.; Chen, L.; et al. Ultrahigh Thermoelectric Performance by Electron and Phonon Critical Scattering in $Cu_2Se_{1-X}I_x$. *Adv. Mater.* **2013**, *25*, 6607–6612. [CrossRef] [PubMed]
21. Liu, H.; Shi, X.; Kirkham, M.; Wang, H.; Li, Q.; Uher, C.; Zhang, W.; Chen, L. Structure-Transformation-Induced Abnormal Thermoelectric Properties in Semiconductor Copper Selenide. *Mater. Lett.* **2013**, *93*, 121–124. [CrossRef]
22. Yu, B.; Liu, W.; Chen, S.; Wang, H.; Wang, H.; Chen, G.; Ren, Z. Thermoelectric Properties of Copper Selenide with Ordered Selenium Layer and Disordered Copper Layer. *Nano Energy* **2012**, *1*, 472–478. [CrossRef]
23. Dennler, G.; Chmielowski, R.; Jacob, S.; Capet, F.; Roussel, P.; Zastrow, S.; Nielsch, K.; Opahle, I.; Madsen, G.K.H. Are Binary Copper Sulfides/Selenides Really New and Promising Thermoelectric Materials? *Adv. Energy Mater.* **2014**, *4*, 1301581. [CrossRef]
24. Bohra, A.; Bhatt, R.; Bhattacharya, S.; Basu, R.; Ahmad, S.; Singh, A.; Aswal, D.K.; Gupta, S.K. Study of Thermal Stability of Cu_2Se Thermoelectric Material. *AIP Conf. Proc.* **2016**, *1731*, 110010. [CrossRef]
25. Brown, D.R.; Day, T.; Caillat, T.; Snyder, G.J. Chemical Stability of $(Ag, Cu)_2Se$: A Historical Overview. *J. Electron. Mater.* **2013**, *42*, 2014–2019. [CrossRef]
26. Bohra, A.K.; Bhatt, R.; Singh, A.; Bhattacharya, S.; Basu, R.; Bhatt, P.; Navaneethan, M.; Sarkar, S.K.; Anwar, S.; Muthe, K.P.; et al. Stabilizing Thermoelectric Figure-of-Merit of Superionic Conductor Cu_2Se through W Nanoinclusions. *Phys. Status Solidi (RRL) Rapid Res. Lett.* **2020**, *14*, 2000102. [CrossRef]
27. Bailey, T.P.; Hui, S.; Xie, H.; Olvera, A.; Poudeu, P.F.P.; Tang, X.; Uher, C. Enhanced ZT and Attempts to Chemically Stabilize Cu_2Se via Sn Doping. *J. Mater. Chem. A Mater.* **2016**, *4*, 17225–17235. [CrossRef]
28. Zhang, R.; Pei, J.; Han, Z.; Wu, Y.; Zhao, Z.; Zhang, B. Optimal Performance of Cu1.8S1−xTex Thermoelectric Materials Fabricated via High-Pressure Process at Room Temperature. *J. Adv. Ceram.* **2020**, *9*, 535–543. [CrossRef]
29. Mikuła, A.; Mars, K.; Nieroda, P.; Rutkowski, P. Copper Chalcogenide–Copper Tetrahedrite Composites—A New Concept for Stable Thermoelectric Materials Based on the Chalcogenide System. *Materials* **2021**, *14*, 2635. [CrossRef]
30. Ge, Z.H.; Chong, X.; Feng, D.; Zhang, Y.X.; Qiu, Y.; Xie, L.; Guan, P.W.; Feng, J.; He, J. Achieving an Excellent Thermoelectric Performance in Nanostructured Copper Sulfide Bulk via a Fast Doping Strategy. *Mater. Today Phys.* **2019**, *8*, 71–77. [CrossRef]
31. Barman, S.K.; Huda, M.N. Stability Enhancement of Cu_2S against Cu Vacancy Formation by Ag Alloying. *J. Phys. Condens. Matter* **2018**, *30*, 165701. [CrossRef]
32. Shi, D.L.; Geng, Z.M.; Shi, L.; Li, Y.; Lam, K.H. Thermal Stability Study of Cu1.97Se Superionic Thermoelectric Materials. *J. Mater. Chem. C Mater.* **2020**, *8*, 10221–10228. [CrossRef]

33. Nunna, R.; Qiu, P.; Yin, M.; Chen, H.; Hanus, R.; Song, Q.; Zhang, T.; Chou, M.-Y.; Agne, M.T.; He, J.; et al. Ultrahigh Thermoelectric Performance in Cu_2Se-Based Hybrid Materials with Highly Dispersed Molecular CNTs. *Energy Environ. Sci.* **2017**, *10*, 1928–1935. [CrossRef]
34. Li, M.; Islam, S.M.K.N.; Yahyaoglu, M.; Pan, D.; Shi, X.; Chen, L.; Aydemir, U.; Wang, X. Ultrahigh Figure-of-merit of Cu_2 Se Incorporated with Carbon Coated Boron Nanoparticles. *InfoMat* **2019**, *1*, 108–115. [CrossRef]
35. Zhou, Z.; Huang, Y.; Wei, B.; Yang, Y.; Yu, D.; Zheng, Y.; He, D.; Zhang, W.; Zou, M.; Lan, J.-L.; et al. Compositing Effects for High Thermoelectric Performance of Cu_2Se-Based Materials. *Nat. Commun.* **2023**, *14*, 2410. [CrossRef] [PubMed]
36. Shen, F.; Zheng, Y.; Miao, L.; Liu, C.; Gao, J.; Wang, X.; Liu, P.; Yoshida, K.; Cai, H. Boosting High Thermoelectric Performance of Ni-Doped Cu1.9S by Significantly Reducing Thermal Conductivity. *ACS Appl. Mater. Interfaces* **2020**, *12*, 8385–8391. [CrossRef] [PubMed]
37. Liu, W.; Shi, X.; Hong, M.; Yang, L.; Moshwan, R.; Chen, Z.G.; Zou, J. Ag Doping Induced Abnormal Lattice Thermal Conductivity in Cu_2Se. *J. Mater. Chem. C Mater.* **2018**, *6*, 13225–13231. [CrossRef]
38. Yue, Z.; Zhou, W.; Ji, X.; Zhang, F.; Guo, F. Enhanced Thermoelectric Properties of Ag Doped Cu_2S by Using Hydrothermal Method. *J. Alloys Compd.* **2022**, *919*, 165830. [CrossRef]
39. Mikuła, A.; Nieroda, P.; Mars, K.; Dąbrowa, J.; Koleżyński, A. Structural, Thermoelectric and Stability Studies of Fe-Doped Copper Sulfide. *Solid. State Ion.* **2020**, *350*, 115322. [CrossRef]
40. Hemathangam, S.; Thanapathy, G.; Muthukumaran, S. Tuning of Band Gap and Photoluminescence Properties of Zn Doped Cu_2S Thin Films by CBD Method. *J. Mater. Sci. Mater. Electron.* **2016**, *27*, 2042–2048. [CrossRef]
41. Emegha, J.O.; Ukhurebor, K.E.; Aigbe, U.O.; Damisa, J.; Babalola, A.V. Synthesis and Characterization of Copper Zinc Iron Sulphide (CZFS) Thin Films. *Heliyon* **2022**, *8*, e10331. [CrossRef]
42. Chetty, R.; Bali, A.; Mallik, R.C. Tetrahedrites as Thermoelectric Materials: An Overview. *J. Mater. Chem. C Mater.* **2015**, *3*, 12364–12378. [CrossRef]
43. Ballikaya, S.; Chi, H.; Salvador, J.R.; Uher, C. Thermoelectric Properties of Ag-Doped Cu_2Se and Cu_2Te. *J. Mater. Chem. A Mater. Energy Sustain.* **2013**, *1*, 12478–12484. [CrossRef]
44. Wang, X.B.; Qiu, P.F.; Zhang, T.S.; Red, D.D.; Wu, L.H.; Shi, X.; Yang, L.H.; Chen, L.D. Compounds Defects and Thermoelectric Properties in Ternary CuAgSe-Based Materials. *J. Mater. Chem. A Mater. Energy Sustain.* **2015**, *3*, 13662–13670. [CrossRef]
45. Hong, A.J.; Li, L.; Zhu, H.X.; Zhou, X.H.; He, Q.Y.; Liu, W.S.; Yan, Z.B.; Liu, J.M.; Ren, Z.F. Anomalous Transport and Thermoelectric Performances of CuAgSe Compounds. *Solid. State Ion.* **2013**, *261*, 21–25. [CrossRef]
46. Zhang, J.Y.; Zhu, J.H.; You, L.; Guo, K.; Li, Z.L.; Lin, W.G.; Huang, J.; Luo, J. Enhanced and Stabilized N-Type Thermoelectric Performance in α-CuAgSe by Ni Doping. *Mater. Today Phys.* **2019**, *10*, 100095. [CrossRef]
47. Yu, T.; Ning, S.; Liu, Q.; Zhang, T.; Chen, X.; Qi, N.; Su, X.; Tang, X.; Chen, Z. Balanced High Thermoelectric Performance in N-Type and p-Type CuAgSe Realized through Vacancy Manipulation. *ACS Appl. Mater. Interfaces* **2023**, *15*, 40781–40791. [CrossRef]
48. Wei, T.-R.; Qin, Y.; Deng, T.; Song, Q.; Jiang, B.; Liu, R.; Qiu, P.; Shi, X.; Chen, L. Copper Chalcogenide Thermoelectric Materials. *Sci. China Mater.* **2019**, *62*, 8–24. [CrossRef]
49. Chakrabarti, D.J.; Laughlin, D.E. The Cu-S (Copper-Sulfur) System. *Bull. Alloy Phase Diagr.* **1983**, *4*, 254–271. [CrossRef]
50. Xiao, X.-X.; Xie, W.-J.; Tang, X.-F.; Zhang, Q.-J. Phase Transition and High Temperature Thermoelectric Properties of Copper Selenide $Cu_{2-x}Sex$ ($0 \leq x \leq 0.25$). *Chin. Phys. B* **2011**, *20*, 087201. [CrossRef]
51. Zhao, L.; Wang, X.; Wang, J.; Cheng, Z.; Dou, S.; Wang, J.; Liu, L. Superior Intrinsic Thermoelectric Performance with ZT of 1.8 in Single-Crystal and Melt-Quenched Highly Dense $Cu_{2-x}Se$ Bulks. *Sci. Rep.* **2015**, *5*, 7671. [CrossRef]
52. Cook, W.R. Phase Changes in Cu_2S as a Function of Temperature, Solid State Chemistry. In Proceedings of the 5th Materials Research Symposium, Boston, MA, USA, 1–5 December 1997; pp. 703–712.
53. Nieroda, P.; Leszczyński, J.; Mikuła, A.; Mars, K.; Kruszewski, M.J.; Koleżyński, A. Thermoelectric Properties of Cu_2S Obtained by High Temperature Synthesis and Sintered by IHP Method. *Ceram. Int.* **2020**, *46*, 25460–25466. [CrossRef]
54. Jin, S.H.; Lim, Y.S. Effect of Zn-Doping on the Phase Transition Behavior and Thermoelectric Transport Properties of Cu_2Se. *Korean J. Met. Mater.* **2020**, *58*, 466–471. [CrossRef]
55. Ji, Y.-H.; Ge, Z.-H.; Li, Z.; Feng, J. Enhanced Thermoelectric Properties of Cu1.8Se1−S Alloys Prepared by Mechanical Alloying and Spark Plasma Sintering. *J. Alloys Compd.* **2016**, *680*, 273–277. [CrossRef]
56. He, Y.; Day, T.; Zhang, T.; Liu, H.; Shi, X.; Chen, L.; Snyder, G.J. High Thermoelectric Performance in Non-Toxic Earth- Abundant Copper Sulfide. *Adv. Mater.* **2014**, *26*, 3974–3978. [CrossRef]
57. Arellano-Tánori, O.; Acosta-Enríquez, M.C.; Ochoa-Landín, R.; Iñiguez-Palomares, R.; Mendívil-Reynoso, T.; Flores-Acosta, M.; Castillo, S.J. Copper-Selenide and Copper-Telluride Composites Powders Sintetized by Ionic Exchange. *Chalcogenide Lett.* **2014**, *11*, 13–19.